THE JOURNAL OF PHYSICAL CHEMISTRY Letters

Letter

pubs.acs.org/JPCL

Chemical Instability of Dimethyl Sulfoxide in Lithium−Air Batteries

David G. Kwabi,[†,‡] Thomas P. Batcho,[‡,§] Chibueze V. Amanchukwu,[∥] Nagore Ortiz-Vitoriano,[†,‡] Paula Hammond,[∥] Carl V. Thompson,*[,§] and Yang Shao-Horn*[,†,‡,§]

[†]Department of Mechanical Engineering, [‡]Electrochemical Energy Laboratory, [§]Department of Materials Science & Engineering, and [∥]Department of Chemical Engineering, Massachusetts Institute of Technology, 77 Massachusetts Ave., Cambridge, Massachusetts 02139, United States

Supporting Information

ABSTRACT: Although dimethyl sulfoxide (DMSO) has emerged as a promising solvent for Li−air batteries, enabling reversible oxygen reduction and evolution ($2Li + O_2 \Leftrightarrow Li_2O_2$), DMSO is well known to react with superoxide-like species, which are intermediates in the Li−O_2 reaction, and LiOH has been detected upon discharge in addition to Li_2O_2. Here we show that toroidal Li_2O_2 particles formed upon discharge gradually convert into flake-like LiOH particles upon prolonged exposure to a DMSO-based electrolyte, and the amount of LiOH detectable increases with increasing rest time in the electrolyte. Such time-dependent electrode changes upon and after discharge are not typically monitored and can explain vastly different amounts of Li_2O_2 and LiOH reported in oxygen cathodes discharged in DMSO-based electrolytes. The formation of LiOH is attributable to the chemical reactivity of DMSO with Li_2O_2 and superoxide-like species, which is supported by our findings that commercial Li_2O_2 powder can decompose DMSO to $DMSO_2$, and that the presence of KO_2 accelerates both DMSO decomposition and conversion of Li_2O_2 into LiOH.

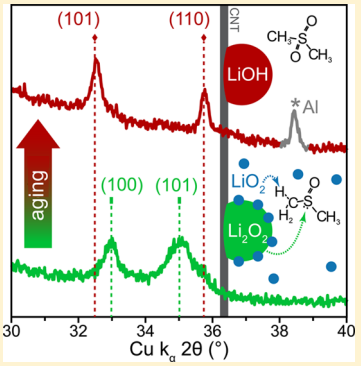

SECTION: Physical Processes in Nanomaterials and Nanostructures

Rechargeable Li−O_2 batteries have received much research attention for their potential to provide higher gravimetric energy than current Li-ion batteries.[1−6] High gravimetric energy gains up to about four times have been shown on the positive electrode basis,[7−10] and a system-level gain of about two times has been projected with the use of metallic lithium and an open system.[3] Despite their promise, significant challenges need to be overcome to make Li−O_2 batteries practical.[1,2,4−6] One of the most prominent challenges is the instability of aprotic electrolytes[11−14] and oxygen electrodes (e.g., carbon[7,15−17]) during the oxygen reduction reaction (ORR) to form Li_2O_2 upon discharge, the oxidation of Li_2O_2 to evolve oxygen upon charge and cycling, which contributes to low round-trip efficiency, poor rate capability, and poor cycle life. The use of dimethyl sulfoxide (DMSO) in Li−O_2 batteries has been shown to increase the solubility of reaction intermediates at the oxygen electrode[18−20] and provide reversible formation of Li_2O_2 for up to ∼100 cycles when combined with nanoporous Au[15] or TiC[17] for the oxygen electrode. However, it is well known that DMSO is susceptible to oxidation by superoxide anions[21] such as in HO_2[22] and KO_2[23,24] and by electrochemical oxidation[24] to produce dimethyl sulfone ($DMSO_2$). Moreover, several recent studies have reported the formation of LiOH in addition to Li_2O_2 with carbon-based cathodes in DMSO-based electrolytes,[19,25−27] where the ratio of Li_2O_2 to LiOH vastly varies among these studies. Although it has been suggested that trace water in aprotic electrolytes containing ether-based solvents can lead to the formation of LiOH[28] via a reaction between Li_2O_2 and water ($Li_2O_2 + 2H_2O \rightarrow 2LiOH + H_2O_2$), a more plausible explanation for the formation of considerable amounts of LiOH upon Li−O_2 cell discharge is the chemical reactivity between species formed in the oxygen electrode upon discharge (e.g., Li_2O_2, solid-state[29−31] and soluble[32] superoxide species) and DMSO. While Sharon et al.[27] have suggested that both Li_2O_2 and superoxide-like species can react with DMSO to form $DMSO_2$ and LiOH, Fourier transform infrared spectroscopy (FT-IR) detects no $DMSO_2$ after 2 months of prolonged exposure of Li_2O_2 to DMSO,[24] and factors that can influence relative amounts of LiOH and Li_2O_2 formed upon discharge of Li−O_2 cells and conditions under which commercial Li_2O_2 powder can react with DMSO to form $DMSO_2$ and LiOH are not completely understood.

In this study, we examine the chemical stability of DMSO upon exposure to electrochemically formed Li_2O_2 on carbon nanotube (CNT) oxygen electrodes and commercial Li_2O_2 with and without KO_2, which acts as source of superoxide anions. We find that toroidal Li_2O_2 particles formed immediately after discharge gradually convert to LiOH upon exposure to the electrolyte, and only LiOH was found upon prolonged exposure (380 h). In addition, gas chromotagraphy with mass spectroscopy (GC−MS) with greater sensitivity than FT-IR measurements clearly revealed the formation of $DMSO_2$

Received: July 2, 2014
Accepted: July 29, 2014
Published: July 29, 2014

   dx.doi.org/10.1021/jz5013824 | J. Phys. Chem. Lett. 2014, 5, 2850−2856

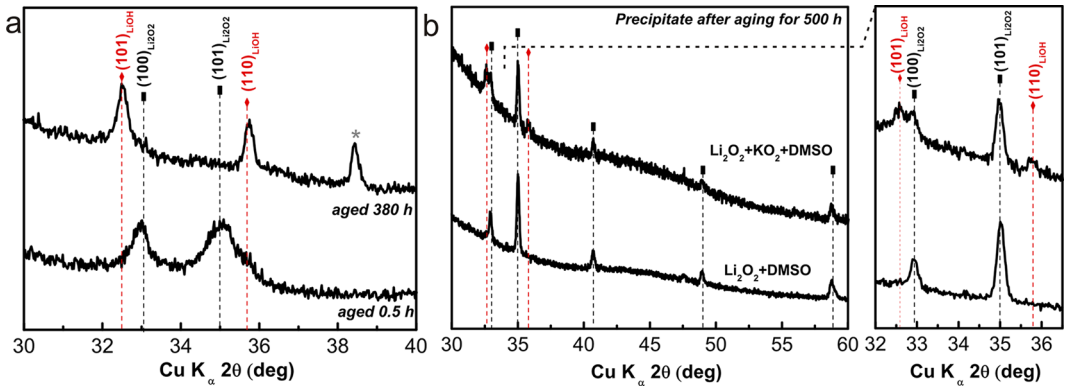

Figure 1. XRD patterns showing evolution of LiOH (red dashed lines) from (a) Li_2O_2 in a CNT electrode discharged at 100 mA/g_C to ~3000 mAh/g_C in 0.1 M $LiClO_4$ in DMSO after 0.5 and 380 h of aging in electrolyte following the completion of discharge. The gray asterisk denotes a peak from the Al substrate. (b) Solid precipitates collected after centrifugation of suspensions containing commercial Li_2O_2, KO_2, and DMSO and Li_2O_2 and DMSO in mole ratios of 1:1:100 and 1:100, respectively, after 500 h of continuous stirring. The magnified section shows major peaks for Li_2O_2 and LiOH.

and thus the chemical instability of DMSO upon prolonged exposure to commercial Li_2O_2 powder. Moreover, the addition of KO_2 to the mixture of DMSO and Li_2O_2 accelerates the formation of LiOH and $DMSO_2$.

We first show that only Li_2O_2 was formed in lab-scale Li−O_2 cells after discharge, which was converted to LiOH in DMSO over time. Figure 1a shows X-ray diffraction (XRD) patterns of CNT-based electrodes discharged at 100 mA/g_C (i.e., 100 mA per gram of CNTs) to ~3000 mAh/g_C and exposed to 0.1 M $LiClO_4$ in DMSO for different amounts of time. While only Li_2O_2 was detected immediately after discharge (i.e., aged 0.5 h), only LiOH was found after 380 h of aging in contact with the electrolyte. It is likely that different resting/aging times for the discharged electrodes between the end of discharge and XRD measurements in previous studies,[19,25−27] which is not reported and not typically monitored, influence the relative amounts of LiOH and Li_2O_2 reported for electrodes discharged in DMSO-based electrolytes.

The conversion of Li_2O_2 to LiOH was accompanied by considerable morphological changes. Toroidal or disc-like Li_2O_2 particles (Figure 2a, marked by small circles) on the order of ~500 nm were found as the majority feature together with a few flake-like particles (Figure 2a, marked by large circles) immediately after discharge in 0.1 M $LiClO_4$ in DMSO. Similar toroidal morphologies have been reported for Li_2O_2 formed in ether-based electrolytes[9,29,30,33−35] upon discharge at low overpotentials (>2.7 V vs Li^+/Li) and current densities. The number of flake-like particles was found to increase (Figure 2b,c) with increasing exposure to the DMSO electrolyte after 12 and 24 h, finally becoming the dominant feature after 576 h (Figure 2d). We attribute these flake-like particles to LiOH based on (i) such particles not being present in pristine CNTs soaked in 0.1 M $LiClO_4$ in DMSO (Figure S1 in the Supporting Information) (ii) XRD results showing the conversion from Li_2O_2 to LiOH with increasing exposure to DMSO (Figure 1), and (iii) energy-dispersive X-ray (EDS) spectroscopy of the flake-like particles, revealing that they were not precipitates from the electrolyte salt (Figure S2 in the Supporting Information). This hypothesis is also supported by recent findings of Xu et al.,[36] which show that the use of a tetramethylene sulfone-based electrolyte suppresses both the formation of flake-like particles *and* the appearance of LiOH as compared with discharge in a DMSO-based electrolyte.

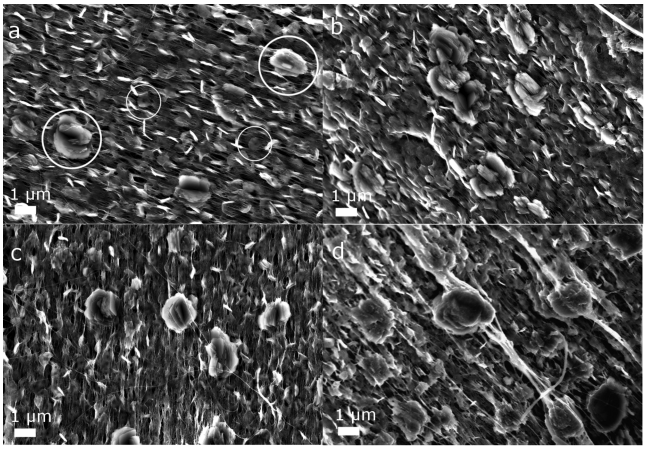

Figure 2. Scanning electron microscopy (SEM) images of CNT electrodes discharged at 25 mA/g_C to ~4000 mAh/g_C in 0.1 M $LiClO_4$ in DMSO imaged (a) 0.5, (b) 12, (c) 24, and (d) 576 h after discharge. Examples of LiOH particles are marked by large circles and examples of Li_2O_2 are marked discs by smaller circles.

The formation of LiOH cannot result from the reactivity between Li_2O_2 and H_2O in the pristine electrolyte as previously proposed[28] as Karl Fischer titration on the pristine electrolyte revealed a water content of 18 ppm, which is ~500 times smaller than the concentration required for direct conversion of discharged Li_2O_2 to LiOH. (See the Supporting Informationfor details of this calculation.) A similar conclusion was reached by Trahan et al.[19] The addition of H_2O from ambient during discharge is negligible because the cell has insignificant cell leakage (~0.5 psi per day), which is supported by the fact that Li_2O_2 is formed invariably upon first discharge[7,29,33] with no LiOH peaks present in XRD (Figure S3 in the Supporting Information) with an electrolyte comprised of 0.1 M $LiClO_4$ in 1,2-dimethoxyethane (DME). This observation is in agreement with previous studies of Li−O_2 cathodes discharged in ether-based electrolytes.[9,11,35] Further support comes from the fact that the Li metal anode in each cell exhibited no signs of corrosion or discoloration after discharge. Therefore, it is proposed that the observed conversion from Li_2O_2 to LiOH in the DMSO-based electrolyte results from the chemical reactivity between DMSO and ORR products. Although both

dx.doi.org/10.1021/jz5013824 | J. Phys. Chem. Lett. 2014, 5, 2850−2856

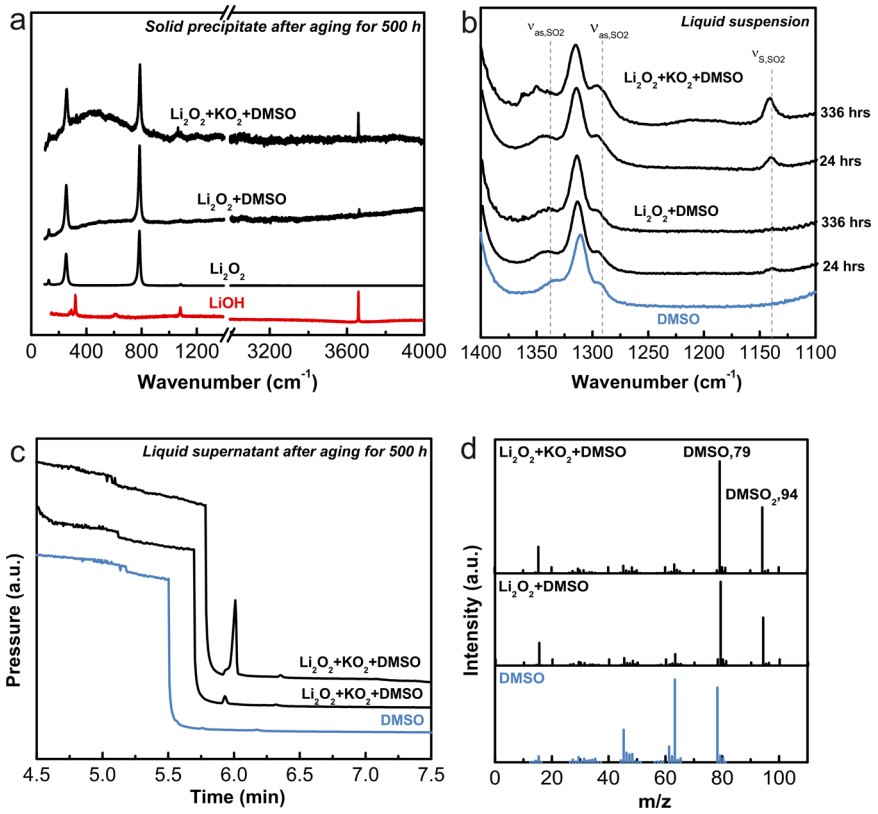

Figure 3. (a) Raman spectra of solid precipitates collected after centrifugation of suspensions of Li_2O_2, KO_2, and DMSO and Li_2O_2 and DMSO in mole ratios of 1:1:100 and 1:100, respectively, after 500 h of continuous stirring. Spectra of commercial Li_2O_2 (ball-milled) and LiOH powders are shown for comparison. Spectra between 3000 and 4000 cm^{-1} have been background-corrected. (See Figure S7 in the Supporting Information.) (b) FT-IR spectra of neat DMSO and suspensions of Li_2O_2, KO_2, and DMSO (with mole ratio of 1:1:100) and Li_2O_2 and DMSO (1:100) after 24 and 336 h of mixing. The peak at 1142 cm^{-1} indicates the symmetric stretch of the SO_2 group in $DMSO_2$. (c) Gas chromatograms showing evolution of column pressure with time of analytes of neat DMSO and supernatants of suspensions of Li_2O_2, KO_2, and DMSO and Li_2O_2 and DMSO in mole ratios of 1:1:100 and 1:100, respectively, after 500 h of continuous mixing and (d) mass spectra of neat DMSO and after ~6 min of analyte evolution for supernatants of suspensions containing Li_2O_2 and DMSO and KO_2, Li_2O_2, and DMSO.

soluble superoxide species and Li_2O_2 have been previously proposed[27] to react with DMSO to form $DMSO_2$ and LiOH, no unique evidence is available to support the chemical reactivity of Li_2O_2 with DMSO because the process of discharging Li−O_2 cells in the previous work[27] can produce both soluble superoxide species and Li_2O_2.

To assess the chemical reactivity of DMSO with Li_2O_2, we examined commercial Li_2O_2 exposed to DMSO with and without superoxide anions in KO_2 present. Two suspensions that contained commercial, ball-milled Li_2O_2 (300 nm to 1 μm) and DMSO in a Li_2O_2/DMSO molar ratio of 1:100 and DMSO with commercial Li_2O_2 and KO_2 in a molar ratio of Li_2O_2/KO_2/DMSO of 1:1:100 were prepared, where KO_2 was used as a source of O_2^- ions. After different amounts of time in the suspension, the liquid components of each suspension were analyzed by FT-IR spectroscopy and GC−MS to identify soluble decomposition products of DMSO, while the solid components were collected after centrifugation of the suspensions, vacuum-dried, and then studied using XRD and Raman spectroscopy.

The addition of KO_2 led to significant conversion of Li_2O_2 to LiOH, which is supported by the appearance of a peak at 3665 cm^{-1} (corresponding to the OH stretch of LiOH[37]) by Raman spectroscopy (Figure 3a). In contrast, while no LiOH was detected by XRD in the solid component from the suspension of Li_2O_2 and DMSO after 500 h (Figure 1b), Raman spectroscopy, which has greater sensitivity to particle surfaces than XRD, revealed a minute amount of LiOH. It is important to note that commercial, ball-milled Li_2O_2 particles were only partially converted to LiOH in DMSO even with KO_2 present for 500 h, in contrast with the complete conversion noted for electrochemically formed Li_2O_2 in the discharged electrodes in DMSO after 380 h in the electrolyte (Figure 1a), indicating greater reactivity of LiO_2 species or electrochemically formed Li_2O_2 than KO_2 toward DMSO. This claim is supported by a recent study in which the presence of a Li^+ salt together with KO_2, causing the generation of LiO_2, was found to promote greater degradation of a number of candidate electrolyte solvents than KO_2 alone.[38] Because commercial Li_2O_2 particles had comparable particle sizes (shown in Figure S4 in the Supporting Information) to electrochemical Li_2O_2 (Figure 2a), higher reactivity of electrochemically formed Li_2O_2 can also be attributed to commercial, ball-milled Li_2O_2 particles having larger crystallite sizes[39] and lower surface concentrations of superoxide[40] than discharged Li_2O_2 toroidal particles, with plate-like crystallites[33] (having largely (001) terminations with LiO_2 surface chemistry[29−31,41]). A recent X-ray photoelectron spectroscopy (XPS) study detected Li_2CO_3 as a byproduct of Li_2O_2 reactivity with DMSO, in addition to LiOH.[42] While Li_2CO_3 was not observed as a decomposition product in this study, it is possible to have Li_2CO_3 on the surface of LiOH particles, such that Li_2CO_3 is not detected by XRD and Raman

dx.doi.org/10.1021/jz5013824 | J. Phys. Chem. Lett. 2014, 5, 2850−2856

spectroscopy, which are much less surface-sensitive than XPS. This hypothesis is supported by our previous work, where a surface layer of Li_2CO_3 was found to exist on commercial LiOH powder.[43]

FT-IR and mass spectrometry analysis shows that the generation of LiOH from Li_2O_2 detected by Raman was accompanied by an increase in $DMSO_2$ in the solution phase. FT-IR spectra of the suspension with KO_2 after 24 h revealed the appearance of a new peak at 1142 cm^{-1}, which was absent in pristine DMSO, as shown in Figure 3b. This peak corresponds to the symmetric stretch of the SO_2 group in $DMSO_2$, and this finding is in agreement with previous work by Mozhzhukhina et al.[24] In contrast, small intensities were found for the $DMSO_2$ peak from the suspension without KO_2 even after 336 h of aging. The presence of $DMSO_2$ in the liquid component from the suspension with KO_2 was further confirmed using GC−MS, which has greater sensitivity than FT-IR and revealed the presence of $DMSO_2$ in the suspension without KO_2 after 500 h of mixing (Figure 3c,d). Gas chromatograms of the supernatants of the suspensions with and without KO_2 displayed a broadened peak, which corresponds to an increase in column pressure, indicative of the production of DMSO (Figure S5 in the Supporting Information). A secondary uptick in pressure after ∼6 min was found for the liquid components from both suspensions with and without KO_2 (Figure 3c), where the peak intensity was much larger in the suspension with KO_2 than the one without. Mass spectra analysis of this peak (Figure 3d) reveals a parent species at an m/z value of 94, which corresponds to the molar mass of $DMSO_2$ at 94.13 g/mol and a fragmentation pattern in good agreement with that reported previously for $DMSO_2$.[44]

The detection of $DMSO_2$ from the liquid component of the suspension without KO_2 and accompanying conversion to LiOH (Figure 3a) shows, for the first time, that DMSO is not stable against Li_2O_2. This finding is further supported by the color change (from milky to yellowish, Figure S6a in the Supporting Information) and FT-IR detection of $DMSO_2$ in a suspension without KO_2 that was mixed with a much higher ratio of Li_2O_2 to DMSO (1:3 molar ratio vs 1:100 previously used) and after a longer time period (1440 h), as shown in Figure S6b in the Supporting Information. This result contrasts with that reported by Mozhzhukhina et al.,[24] who observed no DMSO decomposition when in contact with Li_2O_2 for a comparable 2 month (1440 h) period but do not report the Li_2O_2/DMSO molar ratio used. FT-IR characterization of the higher Li_2O_2/DMSO molar ratio suspension showing the presence of $DMSO_2$ thus highlights the importance of relative concentrations of electrolyte and active material analogues in model chemical reactions to monitor electrolyte decomposition. The greater concentration of $DMSO_2$ in the liquid component from the suspension with KO_2 addition supports the high reactivity of superoxide anions (O_2^-) with DMSO reported previously[23,24,45] and suggests greater reactivity of KO_2 than commercial Li_2O_2 particles with DMSO.

From XRD data showing complete conversion of Li_2O_2 in the discharged CNT cathodes to LiOH, it is clear that the electrochemical discharge product contains species that easily react with DMSO. Controlled studies using suspensions of Li_2O_2 and KO_2 in DMSO suggest that although limited DMSO decomposition occurs in the presence of Li_2O_2 alone, this process is greatly accelerated by the presence of superoxide species and is strongly correlated with the evolution of LiOH. Although, as previously suggested by Mozhzhukhina et al.,[24] nucleophilic attack of DMSO by superoxide can account for $DMSO_2$ evolution (Figure S8a in the Supporting Information), it does not explain LiOH formation. Thus, we propose the following mechanism (Figure S8b in the Supporting Information) as the dominant pathway for LiOH formation and DMSO decomposition: (i) the presence of superoxide promotes proton abstraction from DMSO, resulting in the formation of the dimsyl ion and a free proton and (ii) a Li^+ ion in Li_2O_2 couples strongly to the dimsyl ion and is replaced by the free proton, forming LiOOH, which (iii) then attacks DMSO and forms LiOH and $DMSO_2$. We note that LiOH can itself further decompose DMSO, resulting in the release of water and the formation of lithium methylsulfonate and lithium sulfite species.[27] However, the analysis of solid-state decomposition products by XRD and Raman spectroscopy yielded LiOH only, and no secondary products related to LiOH decomposition. Further studies are required to assess the prominence of the reactivity between LiOH and DMSO.

This proposal is similar to that reported by Sharon et al.,[27] with the important difference that proton abstraction is facilitated by solid-state or near-surface superoxide-related species *after* discharge, in addition to *residual* solution-based superoxide-like intermediates that were formed *during* discharge. This conclusion is obtained from the observation of Li_2O_2 immediately after the end of discharge, before a transformation to LiOH occurs, and is corroborated by the fact that the presence of KO_2 enhances decomposition of commercial Li_2O_2 to LiOH, while Li_2O_2 alone remains relatively stable against DMSO. While solution-based decomposition of DMSO by LiO_2 is possible during discharge, it is important to note that LiO_2 disproportionation (or electron transfer at higher overpotentials) to form solid Li_2O_2 is a competing process.[32] This possibility is borne out by a recent study by Zakharchenko et al.,[46] where the evolution of Li_2O_2 was shown to follow upon the introduction of a Li salt to a suspension of KO_2 in DMSO. Decomposition of DMSO is therefore more likely to proceed by virtue of the presence of superoxide-like species on the surface of solid Li_2O_2, which have been proposed by recent Density Functional Theory (DFT),[31] Raman,[30] magnetic,[41] and X-ray absorption[29] studies in addition to residual LiO_2 species in solution from the ORR. It is important to note that solid-state and soluble forms of superoxide might have different reactivities toward DMSO, which the present study does not distinguish, and further studies will be required to elucidate. We note, however, that recent DFT computations of the energetics of DME-Li_2O_2 cluster interactions suggest that the presence of unpaired spins in Li_2O_2 can lead to hydrogen abstraction from and decomposition of the solvent[47] and that a related interaction may exist between superoxide species and DMSO, whose protons become acidic in the presence of strong bases[48] such as superoxide. Thus, although the very limited evolution of $DMSO_2$ from DMSO in the presence of ball-milled Li_2O_2 may be caused by Li_2O_2 directly,[49] it may also be caused by superoxide-like moieties, which have been proposed to exist on the surface of ball-milled Li_2O_2 particles,[40] rather than Li_2O_2 itself.

An important implication of the time dependence of the chemical instability of DMSO in the presence of superoxide or Li_2O_2 is that short discharge times in lab-scale Li−O_2 batteries using DMSO-based electrolytes will likely result in insignificant DMSO and Li_2O_2 decomposition and thus long cycle life. This is likely the case in previous studies reporting highly reversible

dx.doi.org/10.1021/jz5013824 | J. Phys. Chem. Lett. 2014, 5, 2850−2856

Li_2O_2 formation for ~100 cycles using nanoporous Au[15] and TiC[17] cathodes in DMSO-based electrolytes. On the basis of electrode masses, gravimetric capacities, and current densities provided in refs 15 and 17, we calculate discharge times of 40 min and 1 h 24 min per cycle for nanoporous Au and TiC cathode, respectively. According to the results presented herein, such short exposure times between Li_2O_2 or other discharge intermediates and DMSO are unlikely to result in any significant DMSO decomposition.

In summary, this work presents the time-dependent changes in the discharge product chemistry and morphology of a discharged carbon-based Li−O_2 positive electrode in a DMSO-based electrolyte. We show, for the first time, that Li_2O_2 is the only species detected by XRD immediately after discharge but gradually decomposes completely into LiOH upon prolonged exposure to the electrolyte. Such time-dependent changes after discharge are not typically monitored in Li−air battery research, which can explain previous studies reporting different amounts of Li_2O_2 and LiOH after discharge.[19,25−,27,36] We further show that commercial Li_2O_2 powder can decompose DMSO to $DMSO_2$ and that the presence of KO_2 accelerates DMSO decomposition and the conversion of Li_2O_2 powder into LiOH. These experiments allow us to unambiguously probe the chemical reactivity of DMSO with ORR products, without the influence of carbon electrodes and other species formed during discharge of Li−O_2 cells. While both superoxide-like species[22−24,27] and Li_2O_2[27,49] have been proposed to react and decompose DMSO to $DMSO_2$ and form LiOH, this work is the first to provide unique evidence of the chemical reactivity between DMSO and Li_2O_2. Findings from the work suggest that DMSO might not be suitable for the oxygen electrode in the development of rechargeable Li−air batteries with long cycle life.

EXPERIMENTAL METHODS

Electrochemical Measurements. Li−O_2 cells consisted of a lithium metal anode and freestanding vertically aligned few-walled CNTs (detailed preparation of the nanotubes has been previously reported[7,33]) as the O_2 electrode (~1 × 1 cm). After weighing and vacuum-drying at 100 °C for 8 h, the electrodes were transferred to a glovebox (H_2O < 0.1 ppm, O_2 < 0.1 ppm, Mbraun, USA) without exposure to ambient. Carbon loadings were ~1 mg/cm^2, and all cells were assembled with 0.1 M $LiClO_4$ in DMSO (H_2O < 30 ppm, BASF, USA). Cells were assembled with a lithium foil anode (Chemetall, Germany, 15 mm in diameter) and a Whatman GF/A separator soaked in 120 μL of electrolyte. A stainless-steel mesh was used as the current collector. Following assembly, cells were transferred to a connected second argon glovebox (Mbraun, USA, H_2O < 1 ppm, O_2 < 1%) without exposure to air and purged for 5 min with dry O_2 (99.994 pure O_2, Airgas, H_2O < 2 ppm). After purging, the cells were pressurized to 25 psi (gage) to ensure that an adequate amount of O_2 was available to cells. Electrochemical tests were conducted using a Biologic VMP3. Galvanostatic discharge tests were performed by first resting at open circuit (~2.9 to 3.2 V vs Li^+/Li) for 4 h before applying current.

Ball-Milling of Commercial Li_2O_2. Ball-milling of commercial Li_2O_2 (Sigma-Aldrich, St. Louis, MO) was done in a zirconium oxide milling crucible using a planetary ball mill (Pulverisette 6, Fristch) at 500 rpm for 15 h, reversing every 30 min. Milling reversal was preceded by a 15 min cooling phase. 1 mm zirconia milling balls were dispersed in the Li_2O_2 powder prior to milling.

Mixing of Suspensions Containing Li_2O_2 and KO_2 in DMSO. Mixing of Li_2O_2 (ball-milled) and commercial KO_2 (Sigma-Aldrich) in DMSO was performed in a nitrogen-filled glovebox (H_2O < 0.1 ppm, O_2 < 5 ppm, Mbraun, USA). To obtain a 1:100 Li_2O_2/DMSO ratio, we added 40 mg of commercial (ball-milled) Li_2O_2 to a 20 mL scintillation vial, followed by 6.2 mL of neat DMSO (4 ppm of H_2O). For the experiment involving KO_2, an additional 63 mg of commercial KO_2 was added to another 1:100 Li_2O_2/DMSO mixture to obtain a 1:1:100 molar ratio of Li_2O_2/KO_2/DMSO. The resulting suspensions were stirred using a magnetic stir bar for the duration of the experiment. After 500 h of mixing, each suspension was centrifuged, and the resulting solids were collected and dried under vacuum overnight for analysis by XRD and Raman spectroscopy. The remaining liquid supernatant was analyzed by GC−MS.

X-ray Diffraction Characterization. XRD measurements on electrochemically discharged electrodes were conducted using a Rigaku Smartlab (Rigaku, Salem, NH) in the surface-sensitive parallel beam configuration. For XRD measurements taken immediately after discharge, the CNT electrode was extracted from the Li−O_2 cell immediately after discharge in an argon-filled glovebox and sealed in an airtight XRD sample holder (Anton Paar, Graz, Austria) with a dome that screwed on with a rubber O-ring fitting before being taken to the X-ray diffractometer to minimize exposure to atmospheric contaminants. CNT electrodes that were aged in the electrolyte for extended periods were left in a capped vial together with the separator in an argon-filled glovebox for the desired amount of time before the XRD measurement. Solid precipitates extracted from suspensions containing Li_2O_2 and KO_2 in DMSO were analyzed on a Bruker Advance II diffractometer (Bruker, Billerica, MA) in the conventional Bragg−Brentano geometry. Samples were sealed in an airtight holder (Bruker) with a dome that screwed on with a rubber O-ring fitting to avoid exposure to atmospheric contaminants.

Raman Spectroscopy Measurements. Raman spectroscopy was performed on the solid components of suspensions containing Li_2O_2 with and without KO_2 in DMSO on a LabRAM HR800 microscope (Horiba Jobin Yvon) using an external 20 mW He:Ne 633 nm laser (Horiba, Jobin Yvon), focused with a 50× long working distance objective and a $10^{-0.3}$ neutral density filter. A silicon substrate was used to calibrate the Raman shift.

FT-IR Measurements. FT-IR was used to analyze soluble DMSO decomposition species in suspensions containing Li_2O_2 with and without KO_2 in DMSO. To analyze the mixtures, we deposited 10 μL of each suspension on a transparent KBr Infrared card (International Crystal Laboratories, USA) and removed it from the nitrogen glovebox. A JASCO 4100 Fourier Transform Infrared spectrometer (JASCO Analytical Instruments, USA) was then used at a resolution of 1 cm^{-1} and 100 accumulation scans to perform the measurements.

GC−MS Measurements. GC−MS was used to examine molar masses of solution-based species related to DMSO decomposition. This was carried out on an Agilent 5973 Network Mass Selective detector (Agilent Technologies, Santa Clara, CA). The supernatant obtained from centrifugation of suspensions containing Li_2O_2 with and without KO_2 in DMSO was mixed in excess acetonitrile, which was used as the carrier gas for GC−MS. 1 μL of analyte was injected into the GC inlet, which was heated in progressive stages, beginning

dx.doi.org/10.1021/jz5013824 | J. Phys. Chem. Lett. 2014, 5, 2850−2856

from 100 °C for 5 min to 250 °C for 3 min and, finally, 320 °C for 8 min, ramping between temperature set points at 20 and 30 °C/min, respectively. Mass analysis was performed between 2 and 600 atomic mass units (a.m.u).

SEM Characterization. SEM images were taken using a Zeiss Supra55VP and Ultra55 (Carl Zeiss AG, Germany). Images were taken with an Inlens detector at 5 kV working voltage. To minimize air exposure, we sealed and stored samples in argon before being quickly placed into the SEM chamber. EDS was carried out on the Zeiss Supra 55VP with an EDAX EDS system (Ametek, USA).

■ ASSOCIATED CONTENT

Supporting Information

Additional characterization data. This material is available free of charge via the Internet at http://pubs.acs.org.

■ AUTHOR INFORMATION

Corresponding Authors

*C.V.T.: E-mail: cthomp@mit.edu.

*Y.S.-H.: E-mail: shaohorn@mit.edu.

Notes

The authors declare no competing financial interests.

■ ACKNOWLEDGMENTS

This work was partially supported by the MRSEC Program of the National Science Foundation under award number DMR-0819762, the Robert Bosch Company with a Bosch Energy Research Network Grant, and the CERC−CVC US China Clean Energy Research Center-Clean Vehicles Consortium of the Department of Energy (under award number DE-PI0000012). N.O.-V. was supported by a Marie Curie International Outgoing Fellowship within the seventh European Community Framework Programme (2012). SEM imaging was performed at the Center for Nanoscale Systems (CNS), a member of the National Nanotechnology Infrastructure Network (NNIN), which is supported by the National Science Foundation under NSF award no. ECS-0335765. CNS is part of Harvard University. We acknowledge the assistance of Mr. Joseph Elias, Mr. Thomas Carney, and Mr. Carl Brozek with GC−MS, EDS, and XRD measurements, respectively.

■ REFERENCES

(1) Lu, Y.-C.; Gallant, B. M.; Kwabi, D. G.; Harding, J. R.; Mitchell, R. R.; Whittingham, M. S.; Shao-Horn, Y. Lithium−Oxygen Batteries: Bridging Mechanistic Understanding and Battery Performance. *Energy Environ. Sci.* **2013**, *6*, 750.

(2) Bruce, P. G.; Freunberger, S. A.; Hardwick, L. J.; Tarascon, J.-M. Li-O_2 and Li-S Batteries with High Energy Storage. *Nat. Mater.* **2012**, *11*, 19−29.

(3) Gallagher, K. G.; Goebel, S.; Greszler, T.; Mathias, M.; Oelerich, W.; Eroglu, D.; Srinivasan, V. Quantifying the Promise of Lithium−Air Batteries for Electric Vehicles. *Energy Environ. Sci.* **2014**, *7*, 1555−1563.

(4) Kwabi, D. G.; Ortiz-Vitoriano, N.; Freunberger, S. A.; Chen, Y.; Imanishi, N.; Bruce, P. G.; Shao-Horn, Y. Materials Challenges in Rechargeable Lithium-Air Batteries. *MRS Bull.* **2014**, *39*, 443−452.

(5) Black, R.; Adams, B.; Nazar, L. F. Non-Aqueous and Hybrid Li-O_2 Batteries. *Adv. Energy Mater.* **2012**, *2*, 801−815.

(6) Shao, Y.; Ding, F.; Xiao, J.; Zhang, J.; Xu, W.; Park, S.; Zhang, J.-G.; Wang, Y.; Liu, J. Making Li-Air Batteries Rechargeable: Material Challenges. *Adv. Funct. Mater.* **2013**, *23*, 987−1004.

(7) Gallant, B. M.; Mitchell, R. R.; Kwabi, D. G.; Zhou, J.; Zuin, L.; Thompson, C. V.; Shao-Horn, Y. Chemical and Morphological Changes of Li−O_2 Battery Electrodes upon Cycling. *J. Phys. Chem. C* **2012**, *116*, 20800−20805.

(8) Oh, S. H.; Black, R.; Pomerantseva, E.; Lee, J.-H.; Nazar, L. F. Synthesis of a Metallic Mesoporous Pyrochlore as a Catalyst for Lithium−O_2 Batteries. *Nat. Chem.* **2012**, *4*, 1004−1010.

(9) Wang, Z.-L.; Xu, D.; Xu, J.-J.; Zhang, L.-L.; Zhang, X.-B. Graphene Oxide Gel-Derived, Free-Standing, Hierarchically Porous Carbon for High-Capacity and High-Rate Rechargeable Li-O_2 Batteries. *Adv. Funct. Mater.* **2012**, *22*, 3699−3705.

(10) Mitchell, R. R.; Gallant, B. M.; Thompson, C. V.; Shao-Horn, Y. All-Carbon-Nanofiber Electrodes for High-Energy Rechargeable Li−O_2 Batteries. *Energy Environ. Sci.* **2011**, *4*, 2952.

(11) Freunberger, S. A.; Chen, Y.; Drewett, N. E.; Hardwick, L. J.; Bardé, F.; Bruce, P. G. The Lithium-Oxygen Battery with Ether-Based Electrolytes. *Angew. Chem., Int. Ed. Engl.* **2011**, *50*, 8609−8613.

(12) McCloskey, B. D.; Bethune, D. S.; Shelby, R. M.; Girishkumar, G.; Luntz, A. C. Solvents' Critical Role in Nonaqueous Lithium-Oxygen Battery Electrochemistry. *J. Phys. Chem. Lett.* **2011**, *2*, 1161−1166.

(13) Xu, W.; Hu, J.; Engelhard, M. H.; Towne, S. A.; Hardy, J. S.; Xiao, J.; Feng, J.; Hu, M. Y.; Zhang, J.; Ding, F.; et al. The Stability of Organic Solvents and Carbon Electrode in Nonaqueous Li-O_2 Batteries. *J. Power Sources* **2012**, *215*, 240−247.

(14) McCloskey, B. D.; Valery, A.; Luntz, A. C.; Gowda, S. R.; Wallraff, G. M.; Garcia, J. M.; Mori, T.; Krupp, L. E. Combining Accurate O_2 and Li_2O_2 Assays to Separate Discharge and Charge Stability Limitations in Nonaqueous Li−O_2 Batteries. *J. Phys. Chem. Lett.* **2013**, *4*, 2989−2993.

(15) Peng, Z.; Freunberger, S. A.; Chen, Y.; Bruce, P. G. A Reversible and Higher-Rate Li-O_2 Battery. *Science* **2012**, *337*, 563−566.

(16) Ottakam Thotiyl, M. M.; Freunberger, S. A.; Peng, Z.; Bruce, P. G. The Carbon Electrode in Non-Aqueous Li-O_2 Cells. *J. Am. Chem. Soc.* **2012**, *135*, 494−500.

(17) Ottakam Thotiyl, M. M.; Freunberger, S. A.; Peng, Z.; Chen, Y.; Liu, Z.; Bruce, P. G. A Stable Cathode for the Aprotic Li−O_2 Battery. *Nat. Mater.* **2013**, *12*, 1050−1056.

(18) Laoire, C. O.; Mukerjee, S.; Abraham, K. M.; Plichta, E. J.; Hendrickson, M. A. Influence of Nonaqueous Solvents on the Electrochemistry of Oxygen in the Rechargeable Lithium−Air Battery. *J. Phys. Chem. C* **2010**, *114*, 9178−9186.

(19) Trahan, M. J.; Mukerjee, S.; Plichta, E. J.; Hendrickson, M. A.; Abraham, K. M. Studies of Li-Air Cells Utilizing Dimethyl Sulfoxide-Based Electrolyte. *J. Electrochem. Soc.* **2012**, *160*, A259−A267.

(20) Calvo, E. J.; Mozhzhukhina, N. A Rotating Ring Disc Electrode Study of the Oxygen Reduction Reaction in Lithium Containing Non Aqueous Electrolyte. *Electrochem. Commun.* **2013**, *31*, 56−58.

(21) Frimeh, A. Organic Reactions Involving the Superoxide Anion. In *The Chemistry of Peroxides*; Patai, S., Ed.; John Wiley & Sons, Inc.: Manchester, U.K., 1983; pp 429−461.

(22) Goolsby, A. D.; Sawyer, D. T. Electrochemical Reduction of Superoxide Ion and Oxidation of Hydroxide Ion in Dimethyl Sulfoxide. *Anal. Chem.* **1968**, *40*, 83−86.

(23) Gampp, H.; Lippard, S. J. Reinvestigation of 18-Crown-6 Ether/potassium Superoxide Solutions in Me_2SO. *Inorg. Chem.* **1983**, *22*, 357−358.

(24) Mozhzhukhina, N.; Méndez De Leo, L. P.; Calvo, E. J. Infrared Spectroscopy Studies on Stability of Dimethyl Sulfoxide for Application in Li-Air Battery. *J. Phys. Chem. C* **2013**, 18375−1830.

(25) Xu, D.; Wang, Z.; Xu, J.; Zhang, L.; Zhang, X. Novel DMSO-Based Electrolyte for High Performance Rechargeable Li-O_2 Batteries. *Chem. Commun. (Cambridge, U. K.)* **2012**, *48*, 6948−6950.

(26) Sun, B.; Munroe, P.; Wang, G. Ruthenium Nanocrystals as Cathode Catalysts for Lithium-Oxygen Batteries with a Superior Performance. *Sci. Rep.* **2013**, *3*, 1−7.

(27) Sharon, D.; Afri, M.; Noked, M.; Garsuch, A.; Frimer, A. A.; Aurbach, D. Oxidation of Dimethyl Sulfoxide Solutions by Electro-

chemical Reduction of Oxygen. *J. Phys. Chem. Lett.* **2013**, *4*, 3115−3119.
(28) Meini, S.; Piana, M.; Tsiouvaras, N.; Garsuch, A.; Gasteiger, H. A. The Effect of Water on the Discharge Capacity of a Non-Catalyzed Carbon Cathode for Li-O_2 Batteries. *Electrochem. Solid-State Lett.* **2012**, *15*, A45.
(29) Gallant, B. M.; Kwabi, D. G.; Mitchell, R. R.; Zhou, J.; Thompson, C.; Shao-Horn, Y. Influence of Li_2O_2 Morphology on Oxygen Reduction and Evolution Kinetics in Li-O_2 Batteries. *Energy Environ. Sci.* **2013**, *6*, 2518−2528.
(30) Yang, J.; Zhai, D.; Wang, H.-H.; Lau, K. C.; Schlueter, J. A.; Du, P.; Myers, D. J.; Sun, Y.-K.; Curtiss, L. A.; Amine, K. Evidence for Lithium Superoxide-like Species in the Discharge Product of a Li-O_2 Battery. *Phys. Chem. Chem. Phys.* **2013**, *15*, 3764−3771.
(31) Hummelshøj, J. S.; Luntz, a C.; Nørskov, J. K. Theoretical Evidence for Low Kinetic Overpotentials in Li-O_2 Electrochemistry. *J. Chem. Phys.* **2013**, *138*, 034703.
(32) Peng, Z.; Freunberger, S. A.; Hardwick, L. J.; Chen, Y.; Giordani, V.; Bardé, F.; Novák, P.; Graham, D.; Tarascon, J.-M.; Bruce, P. G. Oxygen Reactions in a Non-Aqueous Li^+ Electrolyte. *Angew. Chem., Int. Ed.* **2011**, *50*, 6351−6355.
(33) Mitchell, R. R.; Gallant, B. M.; Shao-Horn, Y.; Thompson, C. V. Mechanisms of Morphological Evolution of Li_2O_2 Particles during Electrochemical Growth. *J. Phys. Chem. Lett.* **2013**, *4*, 1060−1064.
(34) Black, R.; Oh, S. H.; Lee, J.-H.; Yim, T.; Adams, B.; Nazar, L. F. Screening for Superoxide Reactivity in Li-O_2 Batteries: Effect on Li_2O_2/LiOH Crystallization. *J. Am. Chem. Soc.* **2012**, *134*, 2902−2905.
(35) Fan, W.; Cui, Z.; Guo, X. Tracking Formation and Decomposition of Abacus-Ball-Shaped Lithium Peroxides in Li−O_2 Cells. *J. Phys. Chem. C* **2013**, 2623−2627.
(36) Xu, D.; Wang, Z.; Xu, J.; Zhang, L.; Wang, L.; Zhang, X. A Stable Sulfone Based Electrolyte for High Performance Rechargeable Li-O_2 Batteries. *Chem. Commun. (Cambridge, U. K.)* **2012**, *48*, 11674−11676.
(37) Krishnamurti, D. The Raman and Infra-Red Spectra of Some Solid Hydroxides. *Proc. - Indian Acad. Sci., Sect. A* **1959**, *50*, 247−253.
(38) Bryantsev, V. S.; Uddin, J.; Giordani, V.; Walker, W.; Addison, D.; Chase, G. V. The Identification of Stable Solvents for Nonaqueous Rechargeable Li-Air Batteries. *J. Electrochem. Soc.* **2012**, *160*, A160−A171.
(39) Harding, J. R.; Lu, Y.-C.; Tsukada, Y.; Shao-Horn, Y. Evidence of Catalyzed Oxidation of Li_2O_2 for Rechargeable Li−air Battery Applications. *Phys. Chem. Chem. Phys.* **2012**, *14*, 10540−10546.
(40) Gerbig, O.; Merkle, R.; Maier, J. Electron and Ion Transport in Li_2O_2. *Adv. Mater.* **2013**, *25*, 3129−3133.
(41) Lu, J.; Jung, H.-J.; Lau, K. C.; Zhang, Z.; Schlueter, J. A.; Du, P.; Assary, R. S.; Greeley, J.; Ferguson, G. A.; Wang, H.-H.; et al. Magnetism in Lithium-Oxygen Discharge Product. *ChemSusChem* **2013**, *6*, 1196−1202.
(42) Younesi, R.; Norby, P.; Vegge, T. A New Look at the Stability of Dimethyl Sulfoxide and Acetonitrile in Li-O_2 Batteries. *ECS Electrochem. Lett.* **2014**, *3*, A15−A18.
(43) Yao, K. P. C.; Kwabi, D. G.; Quinlan, R. A.; Mansour, A. N.; Grimaud, A.; Lee, Y.-L.; Lu, Y.-C.; Shao-Horn, Y. Thermal Stability of Li_2O_2 and Li_2O for Li-Air Batteries: In Situ XRD and XPS Studies. *J. Electrochem. Soc.* **2013**, *160*, A824−A831.
(44) Stein, S. E. Dimethyl Sulfone. http://webbook.nist.gov/cgi/cbook.cgi?ID=C67710&Mask=608.
(45) Chin, D. H.; Chiericato, G.; Nanni, E. J.; Sawyer, D. T. Proton-Induced Disproportionation of Superoxide Ion in Aprotic Media. *J. Am. Chem. Soc.* **1982**, *104*, 1296−1299.
(46) Zakharchenko, T. K.; Kozmenkova, A. Y.; Itkis, D. M.; Goodilin, E. A. Lithium Peroxide Crystal Clusters as a Natural Growth Feature of Discharge Products in Li-O_2 Cells. *Beilstein J. Nanotechnol.* **2013**, *4*, 758−762.
(47) Assary, R. S.; Lau, K. C.; Amine, K.; Sun, Y.-K.; Curtiss, L. A. Interactions of Dimethoxy Ethane With Li_2O_2 Clusters and Likely Decomposition Mechanisms for Li-O_2 Batteries. *J. Phys. Chem. C* **2013**, *117*, 8041−8049.
(48) Butler, J. N. Electrochemistry in Dimethyl Sulfoxide. *J. Electroanal. Chem. Interfacial Electrochem.* **1967**, *14*, 89−116.
(49) Laino, T.; Curioni, A. Chemical Reactivity of Aprotic Electrolytes on a Solid Li_2O_2 Surface: Screening Solvents for Li−air Batteries. *New J. Phys.* **2013**, *15*, 095009.